Rare Metal Materials and Engineering
Volume 49, Issue 6, June 2020
Available online at www.rmme.ac.cn

Science Press

Cite this article as: Rare Metal Materials and Engineering, 2020, 49(6): 1834-1839.

ARTICLE

Preparation of Conductive Ti_3O_5 Shell-coating Nano-Al and Its Electrochemical Performance as Anode Materials for Dual-ion Batteries

Tan Jing[1], **Mao Jian**[1], **Zhang Zhengquan**[2]

[1] Sichuan University, Chengdu 610065, China; [2] Bazhong Yike Carbon Co., Ltd, Bazhong 636600, China

Abstract: Conductive Ti_3O_5 shell-coating nano-Al powder was used to prepare the core-shell structure material of Al@Ti_3O_5; it was used as the anode, mesocarbon microbead (MCMB) was the cathode, and the Al@Ti_3O_5-MCMB dual-ion battery (DIB) was assembled. Results show that the discharge platform of the Al@Ti_3O_5-MCMB DIB is up to 4.5 V; the discharge capacity can reach 130.6 mAh·g^{-1}, and the specific energy density is 278.8 Wh·kg^{-1} at a current rate of 0.5 C (the current rate is based on the theoretical specific capacity of graphite, 1 C corresponds to 372 mAh·g^{-1}). The Al@Ti_3O_5-MCMB DIB shows excellent cyclic stability, and the capacity remains at around 110 mAh·g^{-1} in the process of 1000 times circulating at the current rate of 5 C, with a capacity retention rate of 92.9% after circulation.

Key words: aluminum anode material; core-shell structure; Ti_3O_5; mesocarbon microbead; dual-ion battery

Among the high capacity anode materials, aluminum should be one of the most attractive anode materials for lithium ion battery (LIB). Because it has many advantages as anode materials, such as low cost, high theoretical capacity (2235 mAh·g^{-1} if it forms Li_9Al_4)[1,2], low potential plateau (0.19~0.45 V against Li^+/Li[3]), high electrical conductivity[4] and abundant reserves. However, most batteries with micro-thick aluminum film as the anode exhibit high initial capacity, and it fades rapidly in several cycles. These capacity decay is largely due to the huge volume expansion/shrinkage (~100%) during lithiation/de-lithiation[5]. Therefore, the research on the high capacity anode is mainly to solve the problem of pulverization of anode material caused by the volume expansion/shrinkage. For example, Liu and Li et al[6,7] have shown that creating a core-shell nanostructure may be a very effective solution. Another way is that using carbon layer covering the anode materials to realize the performance of ultra-high capacity and long cycle life[8,9]. Therefore, we believe that this general model should also be applied to the aluminum active core.

Dual-ion battery (DIB) is a novel type of battery developed in recent years, which has safer performance, can operate at a wider voltage window, and is cheaper compared to conventional lithium-ion batteries (LIBs), and both of the cations and anions are involved in battery reactions. Owing to the anion intercalation process typically occurring at a higher potential (about4.5 V vs Li^+/Li) and cation intercalation occurring at a lower potential (below 1.0 V vs Li^+/Li), the operation voltage of DIBs is usually higher than that of conventional LIBs.

The use of metal Al as an anode in DIBs can not only save lithium resources but also increase the capacity of the battery. However, in the process of charging and discharging, the Al-Li alloying reaction will make Al pulverization and make the electrochemical performance of the battery extremely poor. Hence, drawing lessons from Ref.[10], in this work a core-shell structure was reported using conductive Ti_3O_5 coating the surface of nano-Al powder (called Al@Ti_3O_5 in the follows). The Al@Ti_3O_5 serves as the anode material and mesocarbon microbead (MCMB) is used as the cathode to improve the cycling stability and rate performance of a dual-ion battery (DIB). When Al core is coated with Ti_3O_5

Received date: June 28, 2019
Foundation item: Sichuan Science and Technology Program (2019YFG0072)

Corresponding author: Mao Jian, Ph. D., Professor, College of Materials Science and Engineering, Sichuan University, Chengdu 610065, P. R. China, Tel: 0086-28-85404370, E-mail: maojian@scu.edu.cn

shell, even if the Al core pulverizes, the active substance is still confined in the closed Ti_3O_5 shell and will not lose electrical contact with the current collector.

1 Experiment

1.1 Preparation of Al@Ti_3O_5 core-shell nanoparticles

Firstly, the core-shell structure of anatase TiO_2 coating aluminum powder was prepared, called Al@TiO_2. The specific preparation method is as follows. Saturated $TiOSO_4$ solution was prepared by dissolving 0.5 g $TiOSO_4$ and 30.0 g 0.5 mol/L H_2SO_4 in 800 mL deionized water. Then 1.35 g commercial aluminum powders with an average diameter of ~50 nm were added to the saturated $TiOSO_4$ solution. Then the mixture was sonicated for 1.0 h. The even solution was continuously stirred for 5.0 h to make aluminum powders to react fully with saturated $TiOSO_4$ solution. The resultant solution was then filtrated and washed three times by ethanol. The received sample was dried at 70 °C for 12 h in a vacuum oven and then the Al@$TiO(OH)_2$ sample was gained. The Al@$TiO(OH)_2$ sample was calcined at 520 °C for 2.0 h in quartz tube furnace filled with Ar. The final Al@TiO_2 was collected for the following characterization and experiment.

Secondly, the Al@Ti_3O_5 core-shell structure was prepared as follows. 0.5 g Al@TiO_2 powder was added to 100 mL anhydrous ethanol with ultrasonic dispersion for 30 min. The mixed sample was put into the electric thermostatic drying oven, and the alcohol was volatilized at 100 °C for 24 h. The dried samples were calcined at 1100 °C for 4 h in a tube furnace under an atmosphere of argon. The intact Al@Ti_3O_5 core-shell structure was obtained by high-temperature calcination.

1.2 Characterization

The morphology of the sample was characterized by field emission scanning electron microscopy (FE-SEM, Hitachi SU8010) and transmission electron microscope (TEM, Tecnai G2 F20 S-TWIN 200 kV), and the phases of the samples were identified by an X-ray diffraction (XRD) diffractometer (Panytical X'Pert PRO) with Cu Kα1 radiation. Thermogravimetric analysis (TGA, Netzsch STA449F3) was measured from room temperature to 1200 °C at a heating rate of 10 $°C/min^{-1}$ with an argon flow of 80 mL/min. X-ray fluorescence spectrometer (XRF) was used to measure the element content of samples.

1.3 Electrochemical test

CR2025 coin cells were assembled for DIB electrochemical performance characterization using MCMB as a cathode material and Al@Ti_3O_5 as anode materials. To prepare the Al@Ti_3O_5 anode, the Al@Ti_3O_5 powder, conductive acetylene black, polyvinylidene fluoride (PVDF) binder were mixed and grinded at the mass ratio of 8:1:1 with the addition of N-methyl-2-pyrrolidinone (NMP) solvent to form homogeneous slurry. The acquired Al@Ti_3O_5 anode slurry was covered onto aluminum foil and dried at 80 °C for 12 h in a vacuum drying oven. Then it was pressed and punched into circular sheets with 14.2 mm in diameter. The MCMB cathode was obtained by a similar method. MCMB powder (16.0~19.0 um, the specific surface area is 1.0~2.0 $m^2 \cdot g^{-1}$), conductive acetylene black, and polyvinylidene fluoride (PVDF) were mixed at a mass ratio of 8:1:1 and grinded with several drops of NMP solvent to form homogeneous slurry. After overlaying onto Al foil, the MCMB cathode was dried at 80 °C for 12 h in a vacuum drying oven, pressed and punched into circular sheets with 14.2 mm in diameter. The electrolyte (LBC305-01, solvent: EC, EMC, and DMC; solvend: $LiPF_6$; additive: VC) was purchased directly from the CAPCHEM company. Galvanostatic charge/discharge measurements were carried out by a battery test system (LAND CT2001A) at room temperature. As a contrast, DIBs using bulk Al foil anode, micro-sized and nano-sized aluminum powder anode were also assembled and tested similarly.

2 Results and Discussion

2.1 Thermal analysis and XRD results

Fig.1a is TG-DSC curve of Al@$TiO(OH)_2$ heated in argon from 50 °C to 1200 °C at a heating rate of 10 °C/min. The $TiO(OH)_2$ shell firstly undergoes dehydration and sample loss of moisture of ~7 wt% at temperatures of 100~400 °C. Then with continuous heating, one distinct peak is observed, which belongs to the phase transformation of amorphous TiO_2 to anatase (520 °C). Based on the TG-DSC result, the anatase TiO_2 shell can be gained at the calcination temperatures greater than 520 °C in argon.

In order to improve the conductivity of Al@TiO_2 materials, we choose the way of deoxidizing TiO_2 in reducing atmosphere at high temperature to obtain a better conductivity Ti_3O_5 shell. Here, PEG-600 was used as the reducing agent because it can be carbonized at high temperatures, and the resulting carbon can provide reducibility[11]. In the experiment, we found that Ti_3O_5 cannot be obtained by directly mixing Al@$TiO(OH)_2$ with PEG-600 and calcination at 1100 °C, as shown in Fig.1b. The alumina phase appears in the XRD patterns of original nano-sized Al powder, while the peak of Al_2O_3 cannot be found in the XRD patterns of Al@$TiO(OH)_2$, which indicates that, during the preparation of core-shell structure, alumina is almost completely removed, and the Al@$TiO(OH)_2$ shell can prevent aluminum powder from being oxidized in air, and the result is in accordance with Ref.[10]. In Fig.1b, the "1100 °C calcined sample" is directly deoxidized Al@$TiO(OH)_2$ by mixing PEG-600 and calcination at 1100 °C. Unfortunately, we cannot find any diffraction peaks of Ti_3O_5 in the diffraction pattern. On the contrary, diffraction peaks of alumina were observed, because the amorphous TiO_2 formed by $TiO(OH)_2$ is not compact, and under high-temperature calcination, a trace amount of oxygen in the tube furnace can react with the aluminum core to form alumina. Based on the above analysis, we adopted the way of converting amorphous TiO_2 into compact anatase TiO_2 shell

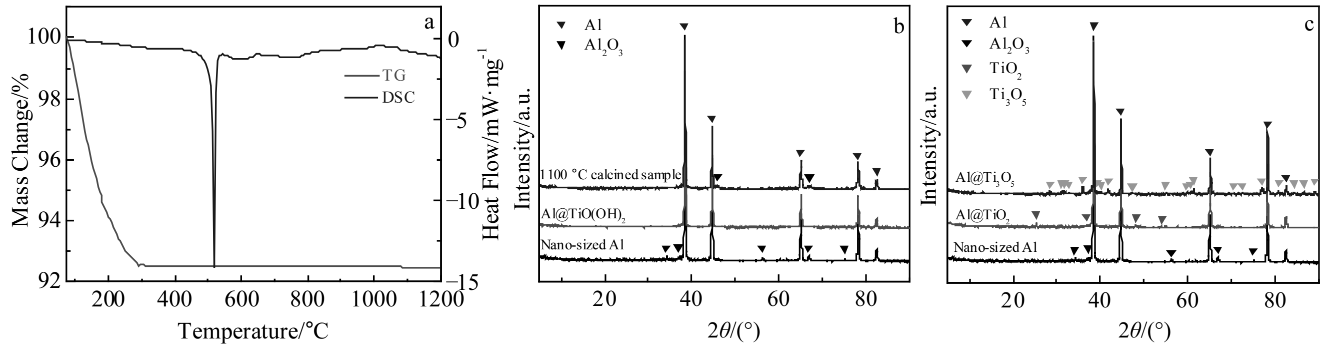

Fig.1 TG-DSC curve of the as-prepared Al@TiO(OH)$_2$ sample heated in argon within 60~1200 °C at a heating rate of 10 °C/min (a); XRD patterns of the nano-sized Al powders, Al@TiO(OH)$_2$ and Al@TiO(OH)$_2$ calcined at 1100 °C for 4 h (b); nano-sized Al powder, as-prepared Al@TiO$_2$ and Al@Ti$_3$O$_5$ samples (c)

firstly, which can better protect the aluminum core from oxidation. And then Al@TiO$_2$ (anatase) was mixed with PEG-600 to gain Ti$_3$O$_5$ by calcination at high temperature. Fig.1c shows the XRD patterns of the as-prepared Al@TiO$_2$ (Al@TiO(OH)$_2$, calcined at 520 °C for 4 h) and as-prepared Al@Ti$_3$O$_5$(Al@TiO$_2$ (anatase) with PEG-600 calcined at 1100 °C for 4 h). In the XRD patterns of Al@TiO$_2$, only the phases of Al and anatase TiO$_2$ are found, which indicates that the outer TiO$_2$ layer effectively protects the inner Al from being oxidized. In the XRD patterns of Al@Ti$_3$O$_5$, there are only phases of Al and Ti$_3$O$_5$, and no Al$_2$O$_3$ peaks can be found. The results show that the outer anatase TiO$_2$ layer can be transformed into Ti$_3$O$_5$, and the compact anatase TiO$_2$ shell can better protect the Al core from oxidation. Therefore, during the experiment, Al@TiO(OH)$_2$ was firstly calcined at 520 °C for 4 h to obtain Al@TiO$_2$ (anatase), and then mixed with PEG-600 and calcined at 1100 °C for 4 h to obtain the Al@Ti$_3$O$_5$.

2.2 Morphology of Al@Ti$_3$O$_5$

Fig.2a shows the SEM image of the as-obtained Al@TiO$_2$ core-shell particles, and we can see the spherical particles with intact structures. Fig.2b is the SEM images of Al@Ti$_3$O$_5$ core-shell particles; it can be seen that after calcination at 1100 °C, the as-prepared Al@Ti$_3$O$_5$ remains intact structure. Fig.2c is the TEM image of Al@Ti$_3$O$_5$, which indicates a complete shell of Ti$_3$O$_5$. In the Al@Ti$_3$O$_5$ core-shell structure, the Al core is completely covered by the outer Ti$_3$O$_5$ shell, and there is a void space between the core and shell that can accommodate the volume expansion of aluminum particle during Al-Li alloying process. Although the Ti$_3$O$_5$ shell is only a few nanometers thick, it can protect the Al core well because of its excellent mechanical stability and anticorrosive properties[12]. Therefore, we would like to deduce the benefits of choosing the Ti$_3$O$_5$ shell: first, in the process of preparing materials in an acidic aqueous solution, it protects the newly formed fresh Al particles in the core; moreover, the Ti$_3$O$_5$ shell not only works as a conductor but also acts as a barrier to prevent Al core from contacting with electrolyte, so the SEI film only forms on the outside surface of the shell.

2.3 Electrochemical performances

In the experiment, Al@Ti$_3$O$_5$ was used as an anode and MCMB as a cathode to assemble Al@Ti$_3$O$_5$-MCMB DIB, and its electrochemical properties are shown in Fig.3. The specific discharge capacities of the DIB were calculated based on the mass of the active material of the MCMB cathode. Fig.3a exhibits the typical charge-discharge curve of the Al@Ti$_3$O$_5$-MCMB DIB at various current rates from 0.5 C (1 C corresponds to 372 mAh·g^{-1}) to 5 C. From the charging and

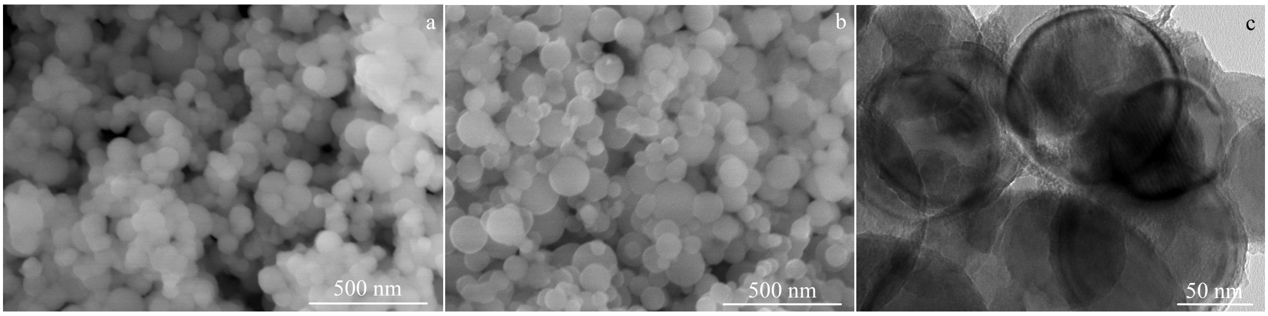

Fig.2 SEM image of the as-obtained Al@TiO$_2$ (a) and Al@Ti$_3$O$_5$ (b) particles; TEM image of Al@Ti$_3$O$_5$ core-shell (c)

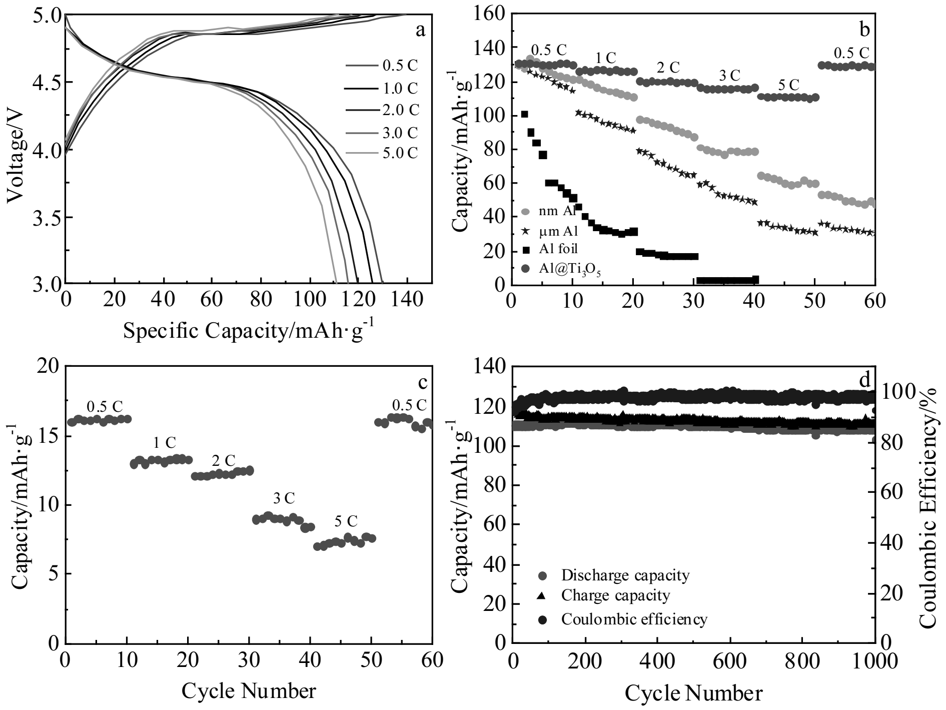

Fig.3 Electrochemical performance of the DIBs over the voltage range of 3~5 V: (a) charge-discharge curves and (b) discharge capacities of the $Al@Ti_3O_5$-MCMB DIB at different current rates; (c) discharge capacities of Ti_3O_5-MCMB DIB; (d) cycling performance of the $Al@Ti_3O_5$-MCMB DIB at 5 C

discharging curve of DIB, it can be seen that its discharge platform is about 4.5 V, and the high discharge platform of DIB makes it have a high energy density. As a contrast, the discharge platform of most aluminum ion batteries (AIBs) is no more than 2 V[13], which severely restricts the energy and power densities of AIBs. At 0.5 C, the discharge capacity is up to 130 $mAh·g^{-1}$. Combined with the high discharge platform (4.5 V), it can get a specific energy density more than 278.8 $Wh·kg^{-1}$, while that of the commercial lithium-ion battery is only 200 $Wh·kg^{-1}$ [14]. Because of the electrochemical polarization at such high current rates, the charge-discharge plateau separation gradually increases with the rise of the current rate, while the charge-discharge profile maintains stability even at 5 C.

Rate performance and high-rate cycling stability are crucial features for batteries applied in high-power applications. Fig.3b shows that when increasing the current rate, the discharge capacity of the $Al@Ti_3O_5$-MCMB DIB remains 130, 126, 120, 116, and 111.4 $mAh·g^{-1}$ at 0.5, 1, 2, 3, and 5 C, respectively. With the increase in the current rate, the discharge capacity goes down slowly. This is in favor of improving the power density of the battery. As a contrast, the capacity of the DIB with nano-Al powder and micron Al powder as anode decays rapidly. For the Al foil-MCMB DIB, the discharge capacity decreases even more severely as the current rate increases.

At the same time, the pure Ti_3O_5 was used as the anode material to assemble the Ti_3O_5-MCMB DIB, and the rate performance of the battery was also tested, and it shows a poor rate performance (Fig.3c). The contents of each element in the as-prepared $Al@Ti_3O_5$ were estimated by XRF, which are 86.6% Al, 7.2% Ti and 6.2% O. According to the capacity of Ti_3O_5-MCMB DIB and the content of Ti in $Al@Ti_3O_5$, it can be concluded that the contribution of Ti_3O_5 shell to the capacity of dual-ion battery is very small.

The cyclic performance (Fig.3d) of the $Al@Ti_3O_5$-MCMB DIB was tested for 1000 cycles at a current rate of 5 C, and the test voltage window is 3~5 V. The discharge capacity is 110 $mAh·g^{-1}$ after 1000 cycles at 5 C with 92.9% capacity retention and over 95.7% coulombic efficiency at a current density of 1860 $mA·g^{-1}$. As a contrast, the common reversible capacity of other DIBs is around 100 $mAh·g^{-1}$ with the current density no more than 200 $mA·g^{-1}$ [15]. As can be seen from Fig.3d, the battery coulombic efficiencies increase with the number of cycles, which is due to the formation of the SEI film on the surface of anode and cathode electrode at the beginning of the cycle, making the battery coulombic efficiencies relatively low. After 100 cycles, the battery shows stable coulombic efficiencies with values of 95.7%.

From the above test results, it can be seen that the DIBs prepared in the experiment have excellent cycle performance and rate performance. The energy density and power density of the DIB are higher than those of the ordinary lithium-ion battery[14], which is determined by the characteristics of the dual-ion battery. The reaction between the anion and the cathode occurs at a higher voltage so the working voltage of the DIB is higher than that of the lithium ion battery, and the high working voltage ensures that the DIB has a high energy density. Moreover, both anion and cation participate in the electrode reaction of cathode and anode at the same time, respectively. That is, during charging, the anion moves to the cathode to participate in the reaction, and meanwhile, the cation moves to the anode to participate in the reaction. During discharge, the anion and cation are removed from the cathode and anode into the electrolyte, respectively. Compared with the LIB, the distance of the ion movement in the DIB is only half of that of LIB. Therefore, the DIB can achieve rapid charge and discharge to improve the power density of the battery.

In order to study the reasons for the excellent cyclic performance of Al@Ti_3O_5-MCMB DIB, the SEM morphology of the anode and cathode of the battery after 1000 cycles was observed, and the results are shown in Fig.4. We can observe that the Al@Ti_3O_5 nanospheres and MCMB microspheres demonstrate no obvious change in morphology after 1000 cycles. The surface of the Ti_3O_5 shell becomes slightly rougher after the charge-discharge cycling (Fig.4b), implying the formation of SEI film. At the same time, in Fig.4c and 4d, we can observe that the MCMB microspheres are almost unchanged after 1000 charge-discharge cycles. Also, no peeling destruction of MCMB is observed in SEM images. The insets in Fig.4c and 4d are the results of EDS element analysis before and after charging, respectively. According to the analysis of element, there is the only element C in MCMB before charging, but elements P, O and F appear after charging, in which the element C comes from MCMB, P and F elements come from anionic PF_6^- in the electrolyte or SEI film formed on the surface of the cathode, and O element comes from SEI film formed on the surface of the cathode. The structure stability of both anode and cathode materials during the long-time cycles at high current rate should be one of the main reasons for its outstanding rate performance and excellent cycling stability.

Electrochemical impedance spectra based on nano-sized Al powders and Al@Ti_3O_5 anodes after 100 cycles within frequency range of 0.01~100 kHz are shown in Fig.4e. The impedance spectra are composed of two depressed semicircles in the high and medium frequency regions and a sloping line in the low frequency regions, which reflect the resistance of the SEI film, the charge transfer resistance and the resistance in Warburg diffusion process, respectively[16]. The Randles equivalent circuit in Fig.4e is used to represent the processes during charge and discharge to help analyze the impedance data. The semicircle in high frequency region is attributed to the formation of SEI film, corresponding to the R_s in the equivalent circuit. The semicircle in medium frequency region is related to the process of charge transfer between electrode and electrolyte, corresponding to the C_{dl} and the R_{ct} in the equivalent circuit. The inclined line in low frequency region is associated with the diffusion of Li^+ in electrode, corresponding

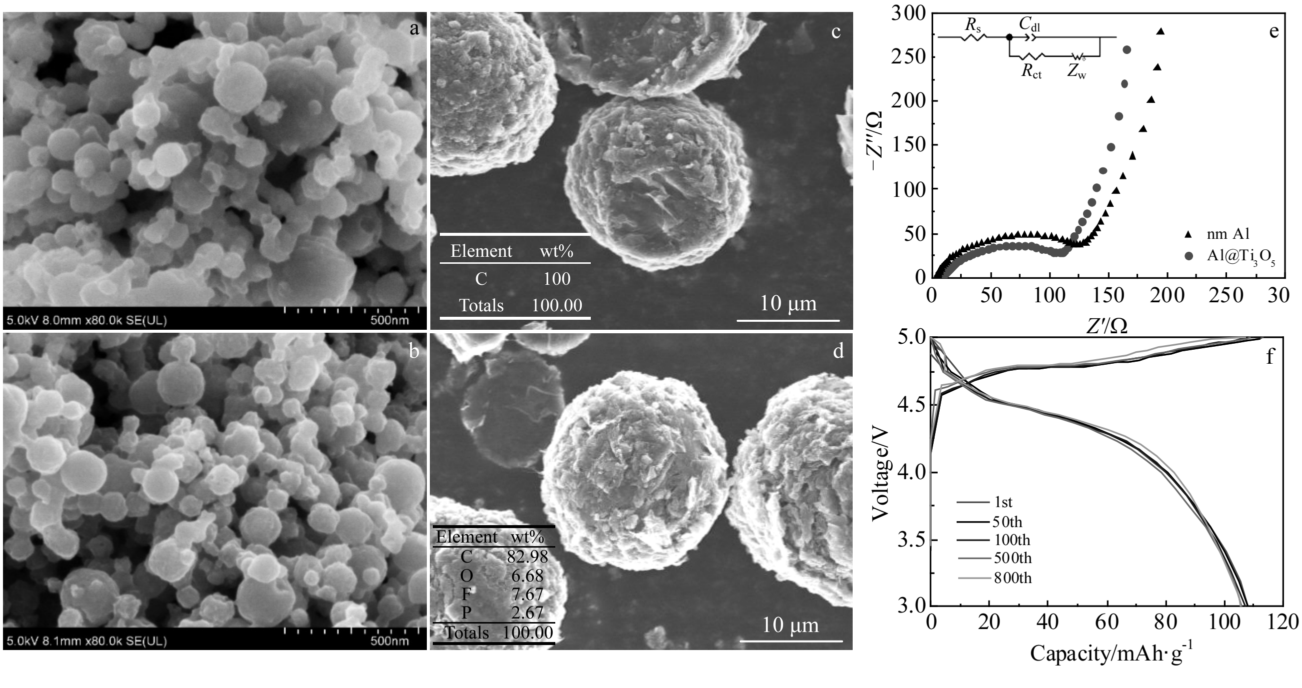

Fig.4 SEM images of the Al@Ti_3O_5 anodes (a, b) and MCMB cathodes (c, d) over the voltage range of 3.0~5.0 V: (a, c) before the charge-discharge cycle and (b, d) after 1000 cycles (5 C); Nyquist plots of DIBs based on nano-Al powder and Al@Ti_3O_5 anode after 100 charge-discharge cycles (5 C) within 0.01~10 mHz (e); charge-discharge curves of the Al@Ti_3O_5-MCMB DIBs at 5 C (f)

to the Z_W in the equivalent circuit. It should be noted that the semicircle of the Al@Ti_3O_5 core-shell structure is smaller than that of the nano-Al, which indicates that the Ti_3O_5 shell can effectively reduce the charge transfer resistance and improve the electrical conductivity. Fig.4f also shows the charge-discharge profiles of the Al@Ti_3O_5-MCMB DIB at 50th, 100th, 500th, and 800th cycles, presenting only a slight polarization.

3 Conclusions

1) Using Al@TiO_2 (anatase) as raw materials and PEG-600 as an additive, through calcining at 1100 °C for 4 h under Ar atmosphere, a core-shell structure Al@Ti_3O_5 composite can be successfully prepared. The core-shell structure consists of aluminum particles completely protected by a thin, conductive and self-supporting Ti_3O_5 shell.

2) A novel Al@Ti_3O_5-mesocarbon microbead (MCMB) dual-ion battery (DIB) is prepared, which shows excellent electrochemical performance and possesses high discharge platform of about 4.5 V, specific energy density of 278.8 Wh·kg^{-1} at 0.5 C, discharge capacity of 110 mAh·g^{-1} with 92.9% capacity retention and high coulombic efficiency (>95.7%) after 1000 cycles at a current density of 1860 mA·g^{-1}. As a contrast, the common reversible capacity of other DIBs is around 100 mAh·g^{-1} with the current density no more than 200 mA·g^{-1}. What's more, instead of using many scarce lithium resources in common LIBs, abundant and low-cost aluminum and titanium are largely used in the novel DIB.

References

1 Gay E C, Vissers D R, Martino F J *et al*. *Journal of the Electrochemical Society*[J], 1976, 123(11): 1591

2 Wen C J, Boukamp B A, Huggins R A *et al*. *Journal of the Electrochemical Society*[J], 1979, 126(12): 2258

3 Nitta N, Yushin G. *Particle & Particle Systems Characterization* [J], 2014, 31(3): 317

4 Wei Feng, Mao Jian, Liu Chunfang *et al*. *Rare Metal Materials and Engineering*[J], 2018, 47(11): 3257

5 Liu Yang, Hudak N S, Huber D L *et al*. *Nano Letters*[J], 2011, 11(10): 4188

6 Liu N, Wu H, Yao Y *et al*. *Nano Letters*[J], 2012, 12(6): 3315

7 Li Weiyang, Zheng Guangyuan. *Nature Communications*[J], 2013, 4: 1331

8 Liu Nian, Wu Hui, Yao Yan *et al*. *Nano Letters*[J], 2012, 12(6): 3315

9 Liu Nian, Lu Zhenda, Zhao Jie *et al*. *Nature Nanotechnology*[J], 2014, 9(3): 187

10 Li Sa, Niu Junjie, Zhao Yucheng *et al*. *Nature Communications* [J], 2015, 6: 7872

11 Chen Yun, Mao Jian. *Journal of Materials Science: Materials in Electronics*[J], 2014, 25(3): 1284

12 Dring K, Dashwood R, Inman D. *Journal of the Electrochemical Society*[J], 2005, 152(3): 104

13 Shyamal K D, Mahapatra S, Homen L. *Journal of Materials Chemistry A*[J], 2017, 5(14): 6347

14 Zhang Xiaolong, Tang Yongbing, Zhang Fan *et al*. *Advanced Energy Materials*[J], 2016, 6(11): 1 502 588

15 Wang Meng, Tang Yongbing. *Advanced Energy Materials*[J], 2018, 8(19): 1 870 088

16 Xu Yuanxian, Li Wenyue, Zhang Fan *et al*. *Journal of Materials Chemistry A*[J], 2016, 4(10): 3697

导电 Ti_3O_5 包覆纳米铝粉的制备及其作为双离子电池负极材料的电化学性能

谭　靖[1]，毛　健[1]，张正权[2]

(1. 四川大学，四川 成都 610065)

(2. 巴中意科碳素股份有限公司，四川 巴中 636600)

摘　要：采用导电的 Ti_3O_5 作为外壳包覆纳米铝粉制备了 Al@Ti_3O_5 核壳结构材料，并将其作为负极材料应用到双离子电池（DIB）中。使用中间相碳微球（MCMB）作为正极材料，Al@Ti_3O_5 作为负极材料制作 Al@Ti_3O_5-MCMB 双离子电池。结果表明，电池的放电平台可达 4.5 V，在电流倍率 0.5 C 下（电流基于正极石墨的理论比容量计算，1 C=372 mAh·g^{-1}）放电比容量达到 130.6 mAh·g^{-1}，比能量密度为 278.8 Wh·kg^{-1}。并且在高倍率 5 C 下循环 1000 次过程中容量基本保持 110 mAh·g^{-1} 不变，循环后容量保持率达到 92.9%。

关键词：铝负极材料；核壳结构；Ti_3O_5；中间相碳微球；双离子电池

作者简介：谭　靖，男，1992 年生，硕士，四川大学材料科学与工程学院，四川 成都 610065，电话：028-85404370，E-mail: TanJing0809@outlook.com